

# Large-Area Triple-Junction a-Si Alloy Production Scale Up

Annual Subcontract Report  
17 March 1992 – 18 March 1993

R. Oswald, J. O'Dowd  
*Solarex Thin Film Division*  
*Newtown, Pennsylvania*

NREL technical monitor: R. Mitchell



**NREL**

**MASTER**

National Renewable Energy Laboratory  
1617 Cole Boulevard  
Golden, Colorado 80401-3393  
A national laboratory operated for  
the U.S. Department of Energy  
under contract No. DE-AC02-83CH10093

Prepared under Subcontract No. ZM-2-11040-2

January 1994

## NOTICE

NOTICE: This report was prepared as an account of work sponsored by an agency of the United States government. Neither the United States government nor any agency thereof, nor any of their employees, makes any warranty, express or implied, or assumes any legal liability or responsibility for the accuracy, completeness, or usefulness of any information, apparatus, product, or process disclosed, or represents that its use would not infringe privately owned rights. Reference herein to any specific commercial product, process, or service by trade name, trademark, manufacturer, or otherwise does not necessarily constitute or imply its endorsement, recommendation, or favoring by the United States government or any agency thereof. The views and opinions of authors expressed herein do not necessarily state or reflect those of the United States government or any agency thereof.

Printed in the United States of America  
Available from:

National Technical Information Service  
U.S. Department of Commerce  
5285 Port Royal Road  
Springfield, VA 22161

Price: Microfiche A01  
Printed Copy A04

Codes are used for pricing all publications. The code is determined by the number of pages in the publication. Information pertaining to the pricing codes can be found in the current issue of the following publications which are generally available in most libraries: *Energy Research Abstracts (ERA)*; *Government Reports Announcements and Index (GRA and I)*; *Scientific and Technical Abstract Reports (STAR)*; and publication NTIS-PR-360 available from NTIS at the above address.



Printed on recycled paper

## **DISCLAIMER**

**Portions of this document may be illegible  
electronic image products. Images are  
produced from the best available original  
document.**

## EXECUTIVE SUMMARY

**Objectives:** The objective of this subcontract over its three-year duration is to advance Solarex's photovoltaic manufacturing technologies, reduce its a-Si:H module production costs, increase module performance and expand the Solarex commercial production capacity. Solarex shall meet these objectives by improving the deposition and quality of the transparent front contact; optimizing the laser patterning process; scaling up the semiconductor deposition process; improving the back contact deposition; and scaling up and improving the encapsulation and testing of its a-Si:H modules. In the Phase I portion of this subcontract Solarex focused on scaling up components of the chemical vapor deposition system for deposition of the front contact, scaling up laser scribing techniques; triple-junction recipes for module production; and metal oxide back contacts. These efforts resulted in adopting portions of the manufacturing line to handle substrates larger than 0.37 m<sup>2</sup>.

### **Task 1: Front Contact Development**

Facilitation of a large-area substrate (0.76 m) (30") chemical vapor deposition (CVD) belt furnace has been completed and an injector has been designed and built. A new gas feed system has been designed and fabricated for both silicon dioxide and textured tin oxide deposition (TTO) including dopant delivery and heated exhaust systems. The uniformity of the coating with the current injector over 0.41 m wide substrates was poor ( $\pm 26\%$ ) on SiO<sub>2</sub>, indicating the need for better injector designs. Simultaneously, other smaller CVD reactors are being utilized to optimize the optical and electrical properties of the tin oxide for triple-junction devices.

### **Task 2: Laser Scribing Process Development**

A large-area (>0.56 m<sup>2</sup>) laser scribing station has been designed and a preliminary system set-up. The aperture area (inside isolation scribe) on these modules with this set-up utilized 86% of the module with future goals of 94% and 96% when scribe

widths and spacings can be reduced. An autofocus system has been designed, built and tested for the large-area laser to accommodate glass warpage and improve laser scribing reliability.

A joint development task between the laser and encapsulation teams have developed a method to pass the wet hi-pot requirement for array modules. New scribing techniques and encapsulants were used to accomplish this task.

Methods to obtain better coupling between the laser beam and the individual substrate layers are under investigation. Utilizing wavelengths other than the standard green (532 nm) has resulted in improved processing speed and more reliable scribes in some applications. Optimization of the parameter space and wavelengths most appropriate for each layer is in progress.

### **Task 3: Amorphous Silicon Based Semiconductor Deposition Process**

The design concept for a five-chamber plasma-enhanced CVD reactor for deposition of  $> 0.56 \text{ m}^2$  triple-junction modules has been completed. A description of some of the detailed features of this system is included in the body of the text. Improvements in the gas distribution, pumping, electrical and substrate heating systems, based on experience with manufacturing systems, have been designed into this large-area multi-chamber reactor.

Optimization of the triple-junction device recipe has proceeded in a separate reactor capable of depositions on  $0.37 \text{ m}^2$  substrates. Initial experiments are underway utilizing  $0.093 \text{ m}^2$  substrates to determine the effectiveness of the recipe transfer and examine overall area uniformity with multiple substrates. The spectral response of films made in this reactor has approached that of the smaller research systems; however, optimization of the diode fill factors is still necessary.

#### **Task 4: Rear Contact Deposition Process**

The efforts in this task have concentrated on the assembly and test of a large-area magnetron sputtering system to deposit the rear contact. A system was partially assembled to test the magnetrons and system design. Several aluminum films were produced and the remainder of the chambers are being assembled in a similar configuration to provide an oxide-metal capability.

A reactive sputtering process for depositing zinc oxide films is under investigation in a small S-gun system capable of multiple metal depositions. A larger manufacturing system is also being utilized to duplicate research optimized coatings on 0.37 m<sup>2</sup> substrates.

#### **Task 5: Bus/Wire/Encapsulation/Frame**

A commercially available indexing system was procured to allow scale-up of the frit dispensing system and an indexer was selected which could fulfill the requirements for both contact dispensing and laser scribing of large-area modules (>0.56 m<sup>2</sup>).

A new auto-refill frit delivery valve is undergoing tests and improvements. This system has allowed larger tolerances to substrate flatness without adversely affecting the deposition thickness, position or width of the bus bar. Evaluations of external connection schemes utilizing both commercially available connectors and new designs are also in progress.

An encapsulant was selected. The encapsulant must provide protection of a thin film through prolonged outdoor exposure and provide a high dielectric path to ground for high voltage protection. Continuous reevaluation, reformulation and accelerated environmental testing have been done to meet these requirements, and even though a potential encapsulant has been selected, further improvement is always necessary.

### **Task 6: Material Handling**

A preliminary equipment layout for a plant with a 10 MW output capacity was completed. The layout was constructed based on input from all task leaders and equipment specialists and is consistent with present practices on our manufacturing line. Vendors of glass handling equipment have been contacted and a manual glass transport system was designed, fabricated and is currently in use.

### **Task 7: Environmental Test, Yield, and Performance Analysis**

Environmental and electrical testing capability of large-area modules is under development by the Task 7 team. The development of a light (1-SUN) soak station capable of uniformly illuminating a 0.56 m<sup>2</sup> area at a constant temperature has been completed. Several more light-soak stations will be constructed to produce a statistical data base for the measurement of stability of large-area multi-junction modules.

Test equipment for the measurement of the environmental durability of large-area modules ( $\geq 0.56$  m<sup>2</sup>) has been reviewed and maintained for optimal test conditions. The equipment currently available includes a hail tester, dry hi-pot tester, humidity-freeze and thermal cycling chambers. A review of the wet hi-pot tester requirements was made with NREL personnel to insure that measurements were consistent. Design and fabrication of a test station for dry/wet hi-pot and edge insulation was completed. Measurements of the breakdown voltages of triple-junction modules with a silver-oxide rear contact have indicated that slightly lower ( $\leq 1$ V) reverse bias voltages can be tolerated to cure small electrical defects. Modification to the fixtures of a standard solar simulator to accommodate both 0.37 m<sup>2</sup> (0.41 m x 0.91 m) and 0.74 m<sup>2</sup> (0.41 m x 1.83 m) modules was completed to allow performance testing of large triple-junction modules.

## TABLE OF CONTENTS

<u>Section</u>	<u>Page</u>
<b>1.0 INTRODUCTION</b> .....	1
<b>2.0 TASK 1: FRONT CONTACT DEVELOPMENT</b> .....	1
2.1 Introduction .....	1
2.2 Large-Area Development .....	1
2.3 Film Property Optimization .....	4
2.3.1 SiO <sub>2</sub> Layer Optimization .....	4
2.3.2 SnO <sub>2</sub> Layer Optimization .....	4
2.3.3 Particulate Reduction Experiments .....	7
2.3.4. Large-Area Tin Oxide Depositions .....	7
<b>3.0 TASK 2: LASER SCRIBING PROCESS DEVELOPMENT</b> .....	8
3.1 Introduction .....	8
3.2 Large-Area Capability .....	9
3.3 Hi-Pot Performance .....	9
3.4 Process Improvement .....	10
<b>4.0 TASK 3: AMORPHOUS SILICON BASED SEMICONDUCTOR DEPOSITION</b> 12	
4.1 Introduction .....	12
4.2 Large-Area Multi-Chamber Deposition System .....	12
4.3 Transfer of Triple-Junction Technology .....	16
4.4 Controlling Shorts with Immediate Metalization .....	18
<b>5.0 TASK 4: REAR CONTACT DEPOSITION PROCESS</b> .....	19
5.1 Introduction .....	19
5.2 Materials Evaluation .....	19
5.3 Large-Area Development .....	20



## TABLE OF CONTENTS CONTINUED

<b>6.0 TASK 5: FRIT/BUS/ENCAPSULATE/FRAME</b> .....	23
6.1 Introduction .....	23
6.2 Large-Area Frit Dispenser .....	23
6.3 Coating .....	25
6.4 Connector .....	28
<b>7.0 TASK 6: MATERIALS HANDLING</b> .....	29
7.1 Introduction .....	29
7.2 Ten Megawatt Plant Layout .....	30
<b>8.0 TASK 7: ENVIRONMENTAL TEST, YIELD AND     PERFORMANCE ANALYSIS</b> .....	30
8.1 Introduction .....	30
8.2 Light-Soak Station .....	30
8.3 Environmental Test .....	35
8.4 Electrical Test .....	37
8.5 Electrical Cure .....	38

## LIST OF FIGURES

<u>Figure</u>		<u>Page</u>
2.1	Deviation in SiO <sub>2</sub> Thickness vs. Location Under Injector . . . . .	3
2.2	Transmission of Standard Tin Oxide, Zinc Oxide and High Transmission Tin Oxide . . . . .	5
2.3	Comparison of Short Circuit Currents Generated by Multi-junction Devices Deposited on Different Types of Tin Oxide . . . . .	6
3.1	Wet Hi-Pot Isolation for Two Scribe Types . . . . .	10
3.2	Interconnect Resistance vs. Natural Log Number of Thermal Cycles . . .	11
4.1	Schematic Diagram of Multi-Chamber a-Si Deposition System . . . . .	13
4.2	a-Si Deposition Chamber . . . . .	14
4.3	Small-Area Triple-Junction Device Made in Large-Area System . . . . .	17
4.4	Quantum Efficiency of Small Area Triple-Junction Device . . . . .	17
4.5	Estimated Response Function of R <sub>S</sub> , PH <sub>3</sub> and B <sub>2</sub> H <sub>6</sub> Factors . . . . .	18
4.6	Shorting Defects as a Function of Delay Before Metalization . . . . .	19
5.1	Schematic Diagram of Magnetron Metalization System . . . . .	21
5.2	Aluminum Thickness vs. Location on Plate . . . . .	22
6.1	Bus-Bar Thickness vs. Working Distance of Tip . . . . .	24
6.2	Wet Hi-Pot Isolation as a Function of Encapsulant . . . . .	26
6.3	Breakdown Voltage vs. Acrylic Thickness . . . . .	27
7.1	10 MW Plant Layout . . . . .	31
8.1	Large-Area Light-Soak Station Layout . . . . .	33
8.2	Impact of Temperature on Light-Induced Effects of a-Si Modules . . . . .	34
8.3	Temperature Map of Light-Soak Station . . . . .	34
8.4	Light-Intensity Map of Light-Soak Station . . . . .	35
8.5	Large-Area Electrical Test Station . . . . .	38
8.6	Manual Electrical Cure of Triple-Junction Modules . . . . .	39
8.7	Automatic Electrical Cure of Triple-Junction Modules . . . . .	40

## LIST OF TABLES

<u>Table</u>	<u>Page</u>
5.1 Effect of Rear Contact on Current Generation .....	20

## **1.0 INTRODUCTION**

Manufacturing large-area multi-junction devices at low cost requires that all component processes be thoroughly investigated for potential cost reductions, durability and capability. Transfer of multi-junction deposition processes from small single or multi-chamber systems to larger reactors requires total re-optimization of recipes and increased attention to deposition uniformity. The repeatability of laser processes must be maintained with the same precision over longer distances often at higher cutting speeds. Chemical vapor deposition (CVD) processes require new injector designs to maintain lateral uniformity of electrical and optical properties. New back contact materials deposited with reactive sputtering techniques need to maintain uniformity to insure reliable laser scribing. Encapsulants must be thoroughly tested environmentally and help provide for safe handling of high voltage interconnected panels. Many of these items have not been addressed in the research efforts to provide high efficiency stable amorphous silicon-alloy devices. Simultaneously, the processes all need to be scaled up to handle larger size modules if cost efficiency goals are to be achieved.

## **2.0 TASK 1: FRONT CONTACT DEVELOPMENT**

### **2.1 Introduction**

The purpose of this task is to scale up the gas delivery system and develop a 0.71 m (28 in) wide injector to be used to deposit a textured tin oxide (TTO) on 0.44 m (16 in) wide substrates using a chemical vapor deposition (CVD) furnace built to our specifications. Our primary emphasis has been on developing the technology required to accomplish this in addition to initiating process experiments designed to optimize the transparent conductive oxide layer for use in multi-junction devices.

### **2.2 Large-Area Development**

In Phase I, the large-area belt furnace has been facilitated with power, water, nitrogen, and the appropriate process and cabinet exhaust systems. In addition, systems for vaporizing liquid feedstocks were designed and tested both in the laboratory and on the large-area CVD furnace. Gas handling systems were designed and installed including a proprietary dopant system which is used to efficiently dope the tin oxide with fluorine. Maintenance areas were set up to handle the cleaning requirements and systems were installed to assure safe operation of the CVD furnace. A computer control system was designed and a manual control system for all process

temperatures and flows was implemented to allow initial system testing and qualification to take place.

Upon the completion of the equipment fabrication and installation, all sub-systems were checked for leaks, calibrated and tested for proper operation. All sub-systems worked very well and the entire system functioned as expected.

The most critical component of a CVD furnace is the injector head assembly. It is the injector that distributes the vaporized chemicals uniformly across the hot substrate inside the furnace; if there is any defect in the injector, it results in a flawed TTO film. Due to the importance of a high quality injector head, three separate paths were explored simultaneously to achieve a useable large-area injector for tin oxide deposition.

#### **Option 1:**

##### **Use/Modify Existing Injector**

An injector was provided by the furnace supplier which had some design and fabrication flaws. This injector represented the furnace supplier's best effort at the time but our testing revealed it to be inadequate for our needs. At best, SiO<sub>2</sub> films deposited using this injector had variations in excess of  $\pm 25\%$ . **Figure 2.1** shows the deviation from the average thickness as a function of position under the injector.

Thickness was measured by depositing SiO<sub>2</sub> on silicon wafers. The deposited oxide was etched to form a step and surface profilometer used to measure its height. Tin oxide films resulted in similar non-uniformities. It was determined that the injector could not be efficiently modified either by us or by its manufacturer to improve its uniformity.

#### **Option 2:**

##### **Purchase the first prototype of a newly designed injector**

The furnace supplier has since developed an improved injector which is radically different from the injector shipped with the furnace. Although a large version of this injector has never been built and tested, it appears to work well on a smaller scale. The drawback of this design is that it is prohibitively expensive, and thus far the

supplier has been unsuccessful in reducing fabrication costs. This option is not viable until the injector costs are lowered by at least 50%.

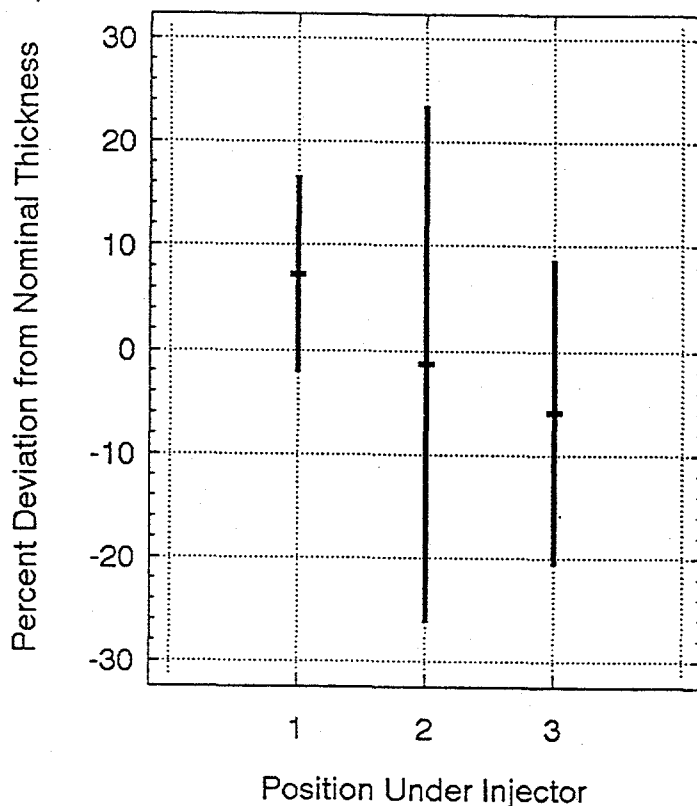


**Figure 2.1.** Deviation in  $\text{SiO}_2$  thickness vs. location under injector. Thickness was measured on 5 wafers for each injector location.

### Option 3:

#### In-House Injector Design

We have successfully designed an injector head based on our own experience with our current manufacturing systems and it appears that we will be able to fabricate our own high quality, reliable injectors at a reasonable cost. A prototype injector has been fabricated and has passed a severe thermal soak test at process temperatures. Final assembly is underway and it is expected that this injector will result in highly uniform TTO films over a .71 m (28") width.

## 2.3 Film Property Optimization

The film properties for the TTO front contact are different for a high efficiency multi-junction device than for our traditional single-junction amorphous silicon structure. Therefore, research has been carried out in an effort to understand the kinetics of the CVD reactions and models have been developed to predict film properties based on process variables. The result of this work will be an optimized TTO front contact. Our efforts this phase have focused primarily on the  $\text{SiO}_2$  layer, the  $\text{SnO}_2$  layer, and particulate generation.

### 2.3.1 $\text{SiO}_2$ Layer Optimization

The large-area CVD furnace was initially set up to deposit  $\text{SiO}_2$  films due to the relative simplicity of the gas delivery system. The  $\text{SiO}_2$  layer was required to block sodium diffusion from the soda-lime glass, and also to provide a chemically pure surface on which to grow the conductive oxide.

Temperature profiles and process parameters were determined for  $\text{SiO}_2$  film deposition at 0.46 m/min (18 in/min) and 0.61 m/min (24 in/min). These films were optimized for uniformity, but due to limitations of the injector head provided by the furnace supplier, the best uniformity achieved was only within 26% of the nominal thickness. While the uniformity was poor, the  $\text{SiO}_2$  layer did prove to be an effective pre-layer for the subsequent deposition of tin oxide.

### 2.3.2 $\text{SnO}_2$ Layer Optimization

In an attempt to understand the reaction kinetics of tin oxide formation in our system, experiments were carried out with the goal of modeling the reaction which would assist us greatly in optimizing the tin oxide for multi-junction devices.

The modeling process was successful and we now have the capability to predict tin oxide properties to within approximately 10-15%. Using this model, process parameters have been developed which have resulted in TTO with significantly higher optical transmission when compared to our current processes. **Figure 2.2** shows the

transmission of this film compared to our standard research quality TTO and zinc oxide films measured in a refractive index matching fluid. It is evident from this graph that this high transmission tin oxide is approaching the very high transmission of our research grade zinc oxide films which have demonstrated significant improvements in cell quantum efficiency.

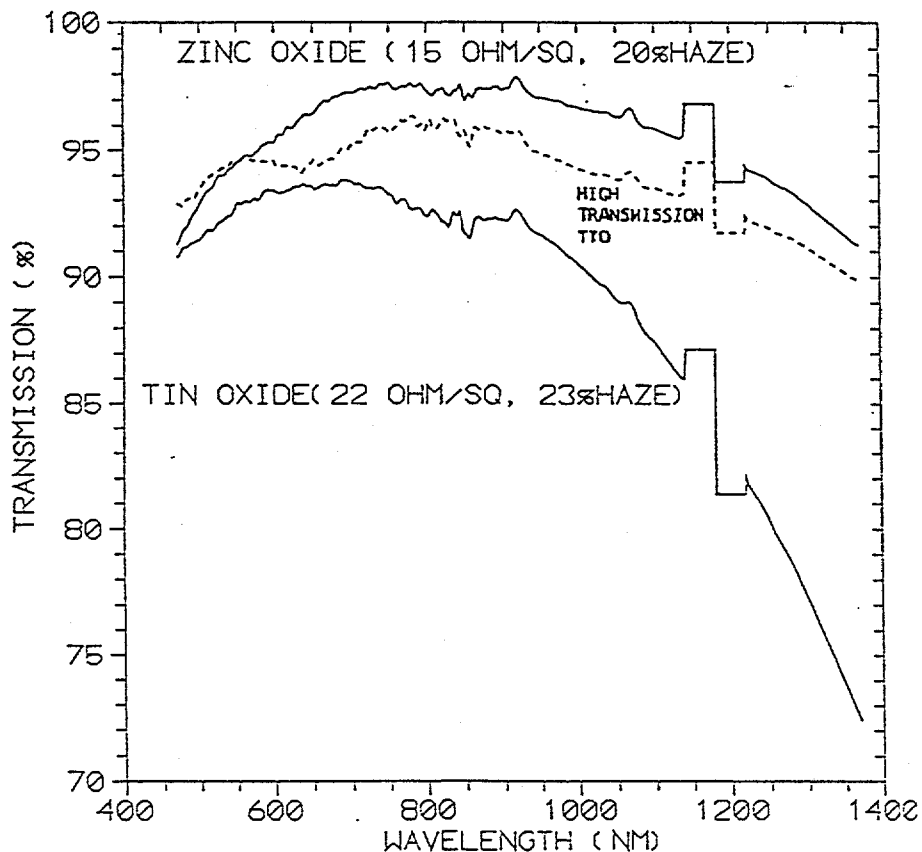


**Figure 2.2.** Transmission of standard tin oxide, zinc oxide, and high transmission tin oxide. Measurements were made using a Perkin-Elmer spectrophotometer with the samples immersed in an index-matching fluid.

An experiment was performed in our silicon deposition system using several types of tin-oxide-coated glass, including the high transmission TTO. Triple-junction structures were deposited on all substrates and the short circuit currents measured; the results



are shown in **Figure 2.3**. Although this is an initial experiment, the data indicates that the high transmission process is clearly better than the standard research grade tin oxide by about 7%.

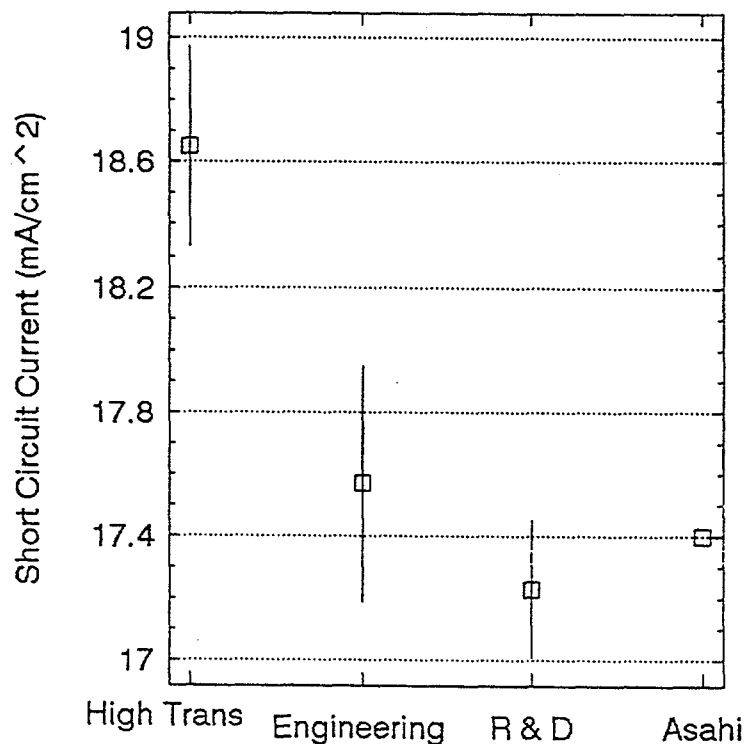


**Figure 2.3.** Comparison of the short circuit currents generated by multi-junction devices deposited on different types of tin oxide.

This same process was successfully transferred to a smaller research CVD furnace where more detailed studies are being carried out. Preliminary results indicate that SiO<sub>2</sub> layer thickness, fluorine concentration, and other reagent concentrations are also very critical in producing high efficiency cells with this high transmission process.

This high transmission process was also adapted to coat our standard soda-lime and low-iron glass substrates.

### **2.3.3 Particulate Reduction Experiments**

One of the problems with atmospheric CVD such as used to make our TTO at Solarex is the incorporation of particles in the growing oxide film. In an effort to identify causes of particulates, a three factor designed experiment was carried out. The three potential causes of particulates studied were: (1) deposition temperature, (2) silane-to-oxygen ratio used in depositing the SiO<sub>2</sub> layer, and (3) use of a vigorous brush wash/rinse in the glass cleaning step. The particles were analyzed and counted using a microscope and classified into "small particles" which were typically less than 15 μm in size and "large particles" which were typically greater than 15 μm.

The results of these experiments show that the factors which had the greatest effect on the "large" particles were deposition temperature and use of a brush-wash and rinse. The higher temperatures tended to cause tin compounds to spall off of the belt and internal surfaces of the furnace, and these particles coated the glass before, during, and after deposition. The brush-wash and rinse prior to deposition was clearly better than a low pressure spray rinse of the glass, and it reduced particles originating from the glass seaming process, as well as the powder-packing materials used between each piece of glass. The silane-to-oxygen ratio had no effect on the number of "large" particles.

None of the factors studied had a large enough effect on "small" particulates to be statistically significant. Typically, the silane-to-oxygen ratio can cause particles of very small size to be deposited in the oxide film in large quantities, but this was not the case during these experiments. In fact, there were very few "small" particles on any of the substrates. While it is encouraging to know that we have almost eliminated our problems with "small" particulates at Solarex, we intend to continue studying the causes of "small" particulate formation to ensure we maintain control of our TTO cleanliness.

### **2.3.4 Large-Area Tin Oxide Depositions**

In order to demonstrate our ability to deposit textured tin oxide over large-areas, we have deposited TTO on both 0.30 m x 1.2 m (12 in. x 48 in.) substrates and 0.41 m x 0.91 m (16 in. x 36 in.) substrates in two CVD furnaces.

The 0.30 m x 1.2 m (12 in. x 48 in.) substrate was coated in our manufacturing CVD furnace using a typical production tin oxide process. This substrate became the deliverable for the contract. These substrates typically have the following properties (as measured in the center):

Sheet Resistance	:	11.3 $\Omega$ /□	
Haze	:	28.1%	
Transmission	:	>80%	In a refractive index matching fluid.

The large-area CVD furnace fabrication was completed just prior to the end of Phase I and we were able to demonstrate that the system was operational by depositing tin oxide on a 0.41 m x 0.91 m (16 in. x 36 in.) substrate. The process has yet to be optimized, and the injector that was provided by the furnace supplier was inadequate for highly uniform TTO; however, the deposit was quite good despite these limitations. The typical properties are:

Sheet Resistance	:	10.3 $\Omega$ /□	
Haze	:	17.0%	
Transmission	:	75%	Measured in air.
Thickness	:	0.8 $\mu$ m	

### 3.0 TASK 2: LASER SCRIBING PROCESS DEVELOPMENT

#### 3.1 Introduction

The laser scribing effort over the past year can be divided into three major areas. The first area of investigation has been the development of large-area scribing capability for all triple-junction device scribes (TTO, silicon, metal, isolation) while increasing scribe rates. The second area involved a joint effort with Task 5 to develop a method of scribing and encapsulation that resulted in a product that passed the wet Hi-pot test. Lastly, studies of new processes that result in better area utilization, reliability, or module efficiency were completed.

### **3.2 Large-Area Capability**

Development of large-area scribing progressed on two fronts. Elements of equipment design were investigated using the vertical scribing system that were incorporated in the design of the new horizontal system. This new system was co-developed by the Task 2 and Task 5 teams and its design meets the combined requirements set forth by each group. This equipment is capable of dispensing the silver frit and of scribing substrates up to 0.41 by 1.8 m in size. Indexing fixtures for both systems have been designed and fabricated. A real-time autofocus system, designed and tested on the vertical lasing system, is being configured for use on the horizontal system. This autofocus will compensate for glass warpage to maintain a constant power density at the glass surface.

These larger-area substrates will require increased scribing rates to maintain economical throughput. The TTO scribe speed was increased from 0.15 m/sec to 0.23 m/sec using an IR (1060 nm.) scribing wavelength. The isolation scribe was increased from 0.06 m/sec to 0.23 m/sec at 1060 nm. The metal scribing step on triple-junction modules was increased under the PVMaT initiative from a rate of 0.05 m/sec to 0.23 m/sec while maintaining module performance criteria.

### **3.3 Hi-Pot Performance**

Solarex has chosen a method of combining a laser isolation scribe with a high dielectric encapsulant to insure the safe operation of large-area modules at array voltages. This is a cost effective way to protect the modules against the corrosive effects of the outdoor environment while simultaneously preventing leakage current to the front surface of the module.

A new type of isolation scribe has been developed which passes dry hi-pot tests on over 96% of the modules tested. This scribe, referred to as the "quad-nine" (4 passes, 0.009 inches wide) can withstand a dry hi-pot test to 1100 volts, before encapsulation. In a similar test of standard isolation scribes, breakdown occurred at 800 volts. The quad-nine also improves wet hi-pot breakdown. As can be seen in **Figure 3.1**, only 18% of the 43 coated modules scribe with the standard isolation survived the wet hi-pot test at 2250 volts. Nearly 70% of the quad-nine scribe plates with the identical encapsulant passed the test.

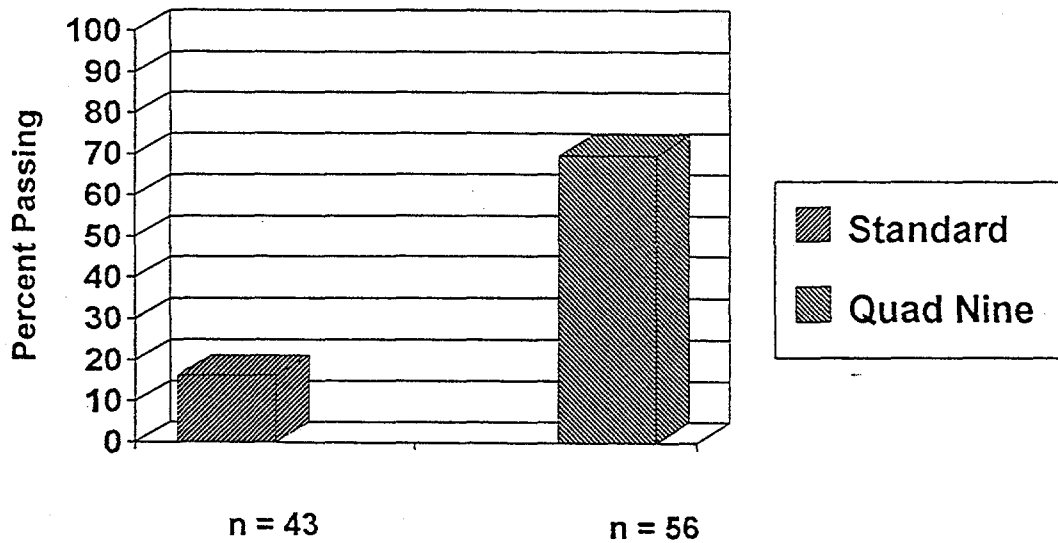


**Figure 3.1.** Wet hi-pot isolation for two different scribe widths. The plates were measured to 2250 volts as per the Interim Qualifications Test. (SERI/TR-213-3624)

Several other techniques have been tried to improve hi-pot resistance without success. Edge seaming of glass substrates was done after the deposition of the transparent front contact without improving hi-pot resistance; and a thin film high dielectric coating deposited on top of the metal back contact layer before the application of the encapsulant, did not increase the resistance to high voltage breakdown in the isolation scribe.

### 3.4 Process Improvement

The effect of different scribe wavelengths and optical delivery equipment was investigated in order to improve the cutting efficiency of the laser and decrease the size of the resulting kerf. As mentioned earlier, infrared scribing improved the scribing rate of both the TTO and isolation scribes. Wavelengths of less than 300 nm were also investigated. These wavelengths yielded poor results for metal scribes, but have shown some promise as a means to interconnect the back metal with the front TTO contact as well as for scribing the TTO.

A study of the reliability of our standard interconnect scheme, which uses a laser weld process, was completed during this phase. The study was undertaken to provide a baseline for the development of a laser weld scribe for use with triple-junction modules and to provide an accelerated testing method for determining the reliability of new scribing techniques. Reliability of the module is compromised by an increase in interconnect resistance resulting from thermal stress of these welds. **Figure 3.2** shows the behavior of the interconnect plotted against the natural log of the number of thermal cycles, which ranged from 233 K to 363 K over a 6 hour period. Preliminary correlation of these data with similar modules placed outside indicate that extrapolating to 700 thermal cycles may give a reasonable estimate for a twenty year value for a module placed outdoors. In any event, the data from the standard process will be used as a baseline in the evaluation of new processes for scribing high efficiency materials.

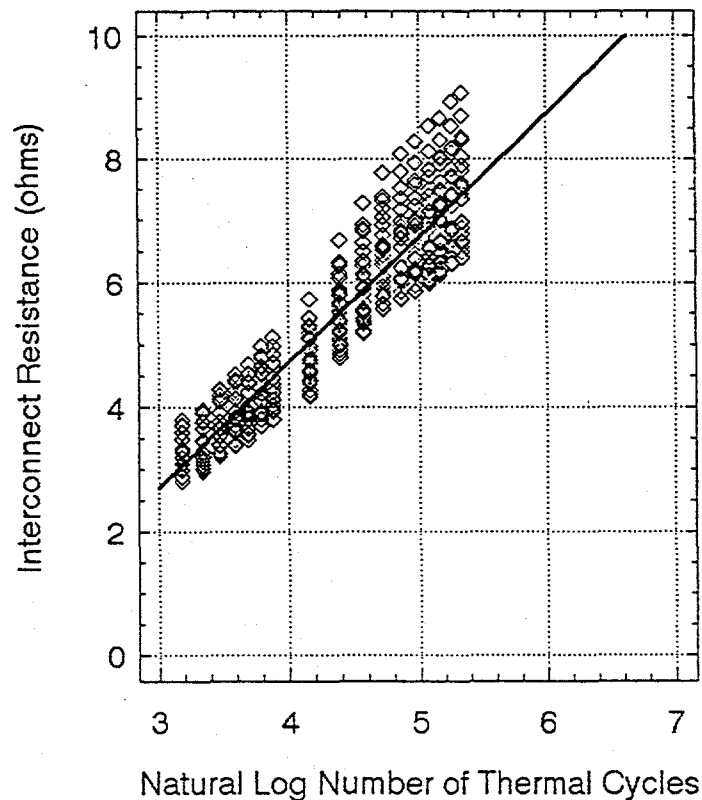


**Figure 3.2.** Interconnect resistance vs. the natural log of the number of thermal cycles. In a cycle, the temperature was varied from 233 K to 363 K over a six hour time period.

## 4.0 TASK 3: AMORPHOUS SILICON BASED SEMICONDUCTOR DEPOSITION

### 4.1 Introduction

Progress was made in the last year on two separate fronts: The design was completed for a five-chamber, large-area deposition system, and the triple-junction technology was transferred from R&D to a large-area single-chamber system.

### 4.2 Large-Area Multi-Chamber Deposition System

The five-chamber system will incorporate many improvements over the existing technology at Solarex:

1. **Capability for deposition on large-area substrates.** The new system will deposit films on substrates up to  $0.74 \text{ m}^2$ , compared to existing manufacturing systems which are limited to just over  $0.1 \text{ m}^2$ . The size of the cathode, which determines the potential area of deposition, will be about twice the size of existing systems.
2. **Multiple deposition chambers.** The new system will have five deposition chambers, compared to two chambers for the existing manufacturing system. This improvement will allow higher throughput with simultaneous depositions in each chamber (see **Figure 4.1**).
3. **"Diode" gas distribution system.** A new gas distribution design will be tested, where the showerhead will be placed very close to the cathode to prevent a glow discharge in the interval between the plates (see **Figure 4.2**). In existing systems, there is deposition on the showerhead and both sides of the cathode, wasting material and creating sources of a-Si flakes which cause pinhole shorts in modules. The "diode" configuration will be an important precursor step towards a "hollow cathode" configuration for a vertical system.

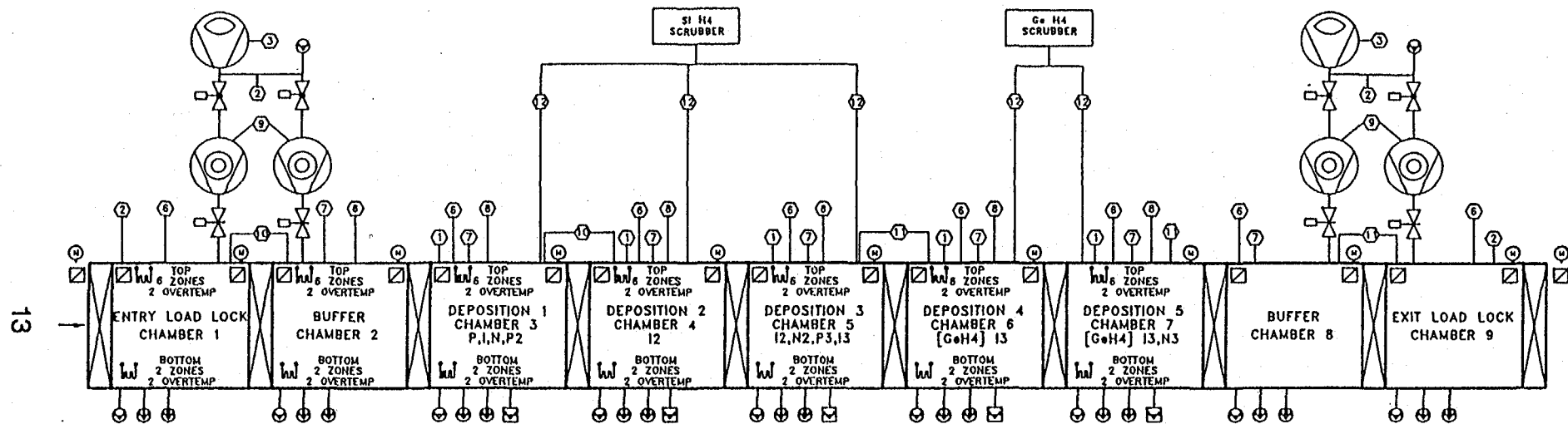


Figure 4.1. Schematic diagram of the multi-chamber a-Si deposition system.



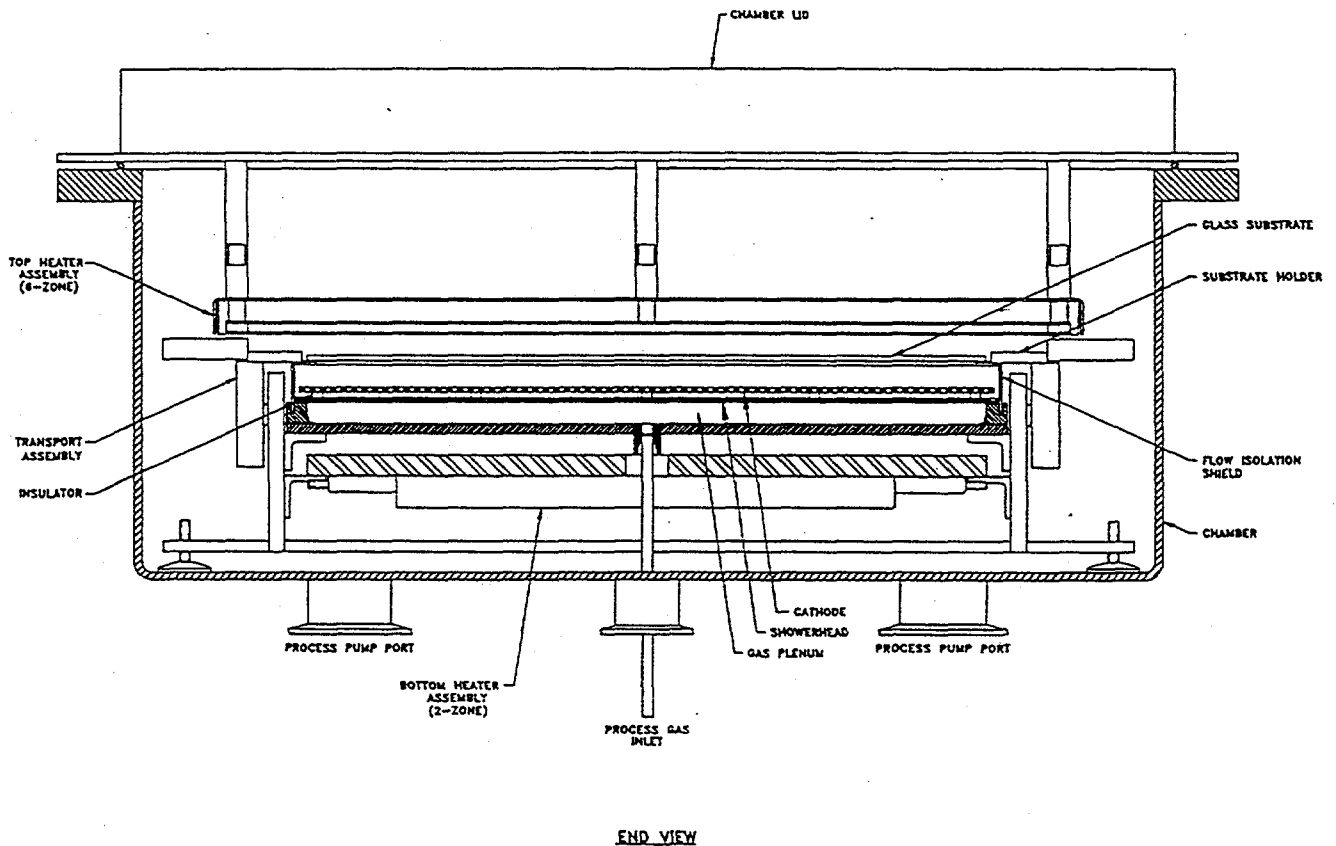


Figure 4.2. The a-Si deposition chamber (cross-sectional view)

4. **Six-zone top heater configuration.** This will ensure good substrate temperature uniformity. Existing systems use a three-zone heater configuration, which results in a drop-off in temperature at the substrate edges.
5. **Alternative cathode materials.** All existing systems use molybdenum for cathodes, and many systems employ molybdenum substrate holders. Molybdenum is very expensive and difficult to machine. The use of alternative materials such as titanium will be explored in the design of the new system.

6. **Symmetrical pumping.** Symmetrical placement of pump ports in the deposition chamber, together with the arrangement of the plenum, showerhead, cathode, and substrate, will ensure a uniform distribution of gas flow across the substrate. This is thought to be particularly important in RF deposition. The existing manufacturing system has some uniformity problems caused by asymmetrically-placed pump ports.
7. **RF capability.** All a-Si deposition systems at Solarex now use DC power supplies, with the exception of a few small systems in R&D. Films made with RF have the potential for better gas utilization and longer times between cleaning because there is less deposition on the cathode. The new system will be designed to incorporate both DC and RF deposition techniques.
8. **Easy cleaning.** The cathode and flow isolation shield are designed to be easily removed for cleaning, saving maintenance labor costs. Internal parts have to be cleaned frequently to prevent flaking of built-up layers of a-Si which can also affect the reliability of the modules produced.
9. **Team design.** The design was reviewed by a team consisting of equipment designers, machinists, electricians, process engineers and research scientists. This cross-departmental team approach gave everyone involved in the task input from the beginning of the project. Not all problems can be anticipated, but giving many people input up-front minimizes risks, and allows the best possible design with the materials at hand.

Chambers purchased from Glasstech Solar are being modified to fit our technology. The chambers have been cleaned and aligned, slit valves installed, and holes cut for exhaust gas pump ports. A 0.12 m<sup>2</sup> titanium cathode was tested in an R&D system, producing good uniformity and high-efficiency devices. Titanium is significantly cheaper than molybdenum. We are also exploring hole-punching instead of drilling in machining the literally thousands of holes needed for the uniform gas distribution over the large-area cathodes. If it works, this is expected to cut machining costs by about 90%.

### 4.3 Transfer of Triple-Junction Technology

The triple-junction technology developed in R&D was transferred to a manufacturing deposition system capable of depositing silicon over  $0.37 \text{ m}^2$  ( $4 \text{ Ft}^2$ ), compared to about  $0.1 \text{ m}^2$  for the R&D systems. This system was formerly used for batch-line manufacturing and was converted to make triple-junctions by expanding the gas-delivery manifold from six gases to nine. Holders have been designed and built for  $0.41 \times 0.91 \text{ m}$  substrates (the original holders took three  $0.1 \text{ m}^2$  ( $12 \times 13 \text{ in.}$  substrates). Uniform depositions have been demonstrated over an area of  $0.37 \text{ m}^2$ .

Work over the first several months focused on matching the best R&D efficiencies for small-area devices. Much time was spent optimizing the thickness and transmission of the non-current-generating P- and N-layers, in order to maximize current generation in the I-layers. A new process had to be developed using diborane in helium as a feedstock gas for P-layers, replacing diborane in silane, which is no longer supplied by gas vendors. Small-area device efficiencies of 9-9.5% have been achieved (see **Figure 4.3**). Integrated QE currents and  $V_{oc}$ 's matched that achieved in R&D (see **Figure 4.4**), but FF's were in the range of 0.63 to 0.66, well below what is needed for efficiencies greater than 10%. Several batches of  $0.1 \text{ m}^2$  modules were made, with the best aperture-area efficiency being 8.3%. Again, low FF was the principle limitation on efficiency.

Results of a three-factor, two-level designed experiment showed that higher dopant gas flows at the second NP junction of triple-junction devices significantly lowered series resistance (see **Figure 4.5**). These changes did not result in higher FF's because of boron contamination of the third I-layer, caused by long residence times of boron in the deposition chamber with high diborane flows. Process changes such as lower deposition temperatures, longer flush times, and flushing with phosphine have ameliorated but not eliminated this problem. The use of microcrystalline I-layers, recently developed in R&D, removes the necessity of using diborane, and boosts FF,  $V_{oc}$ , and transmission. The Glasstech system will have a separate gas delivery manifold for I-layer gases to insure against cross-contamination.

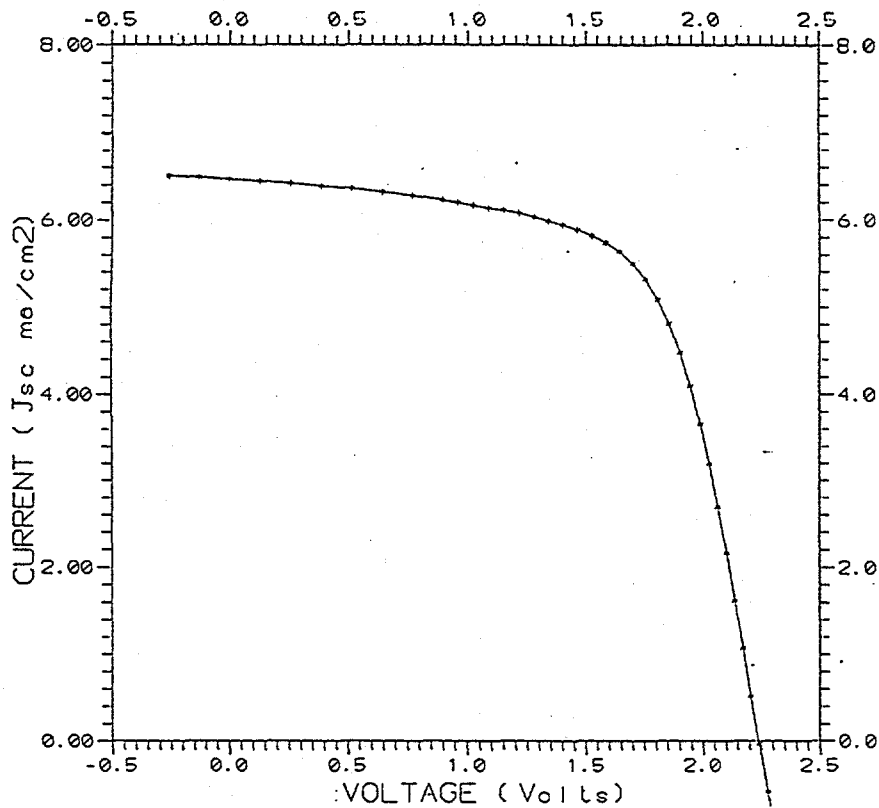


Figure 4.3. IV curve for a small-area triple-junction system.

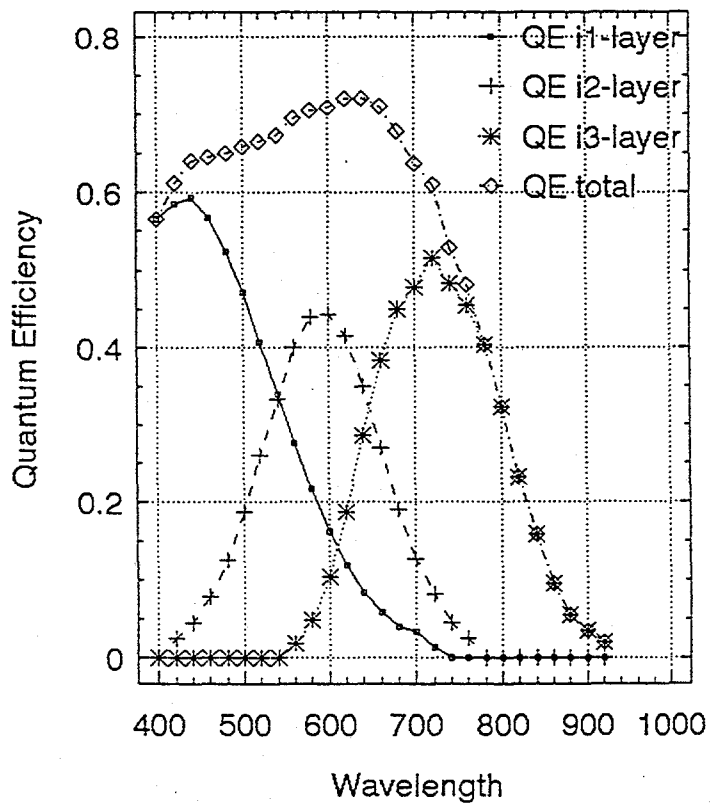
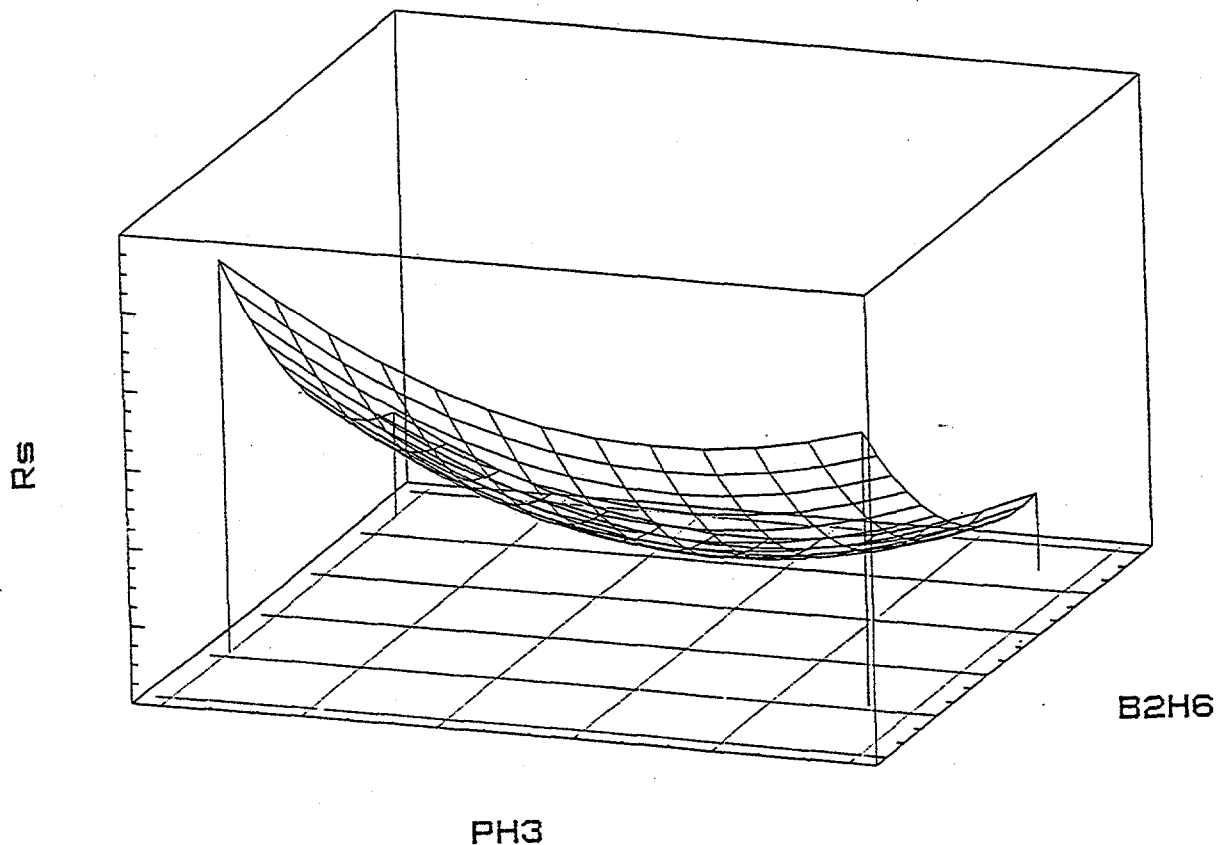


Figure 4.4. The quantum efficiency of a small-area triple-junction device produced in the large-area system.



**Figure 4.5.** The estimated response function of device series resistance using phosphine and diborane flow as factors. The response was generated using data obtained through a screening experiment.

#### 4.4 Controlling shorts with immediate metalization

Shorting is expected to be the biggest source of yield loss for large-area multi-junction modules. An experiment on the Solarex manufacturing line compared the density of active-area defects causing shorts for modules metalized immediately after a-Si deposition in a continuous fabrication process, versus modules where metalization was delayed for several days. The continuous-process modules had about a six-fold decrease in shorting defects, and a much higher percentage of modules with zero defects (see **Figure 4.6**).

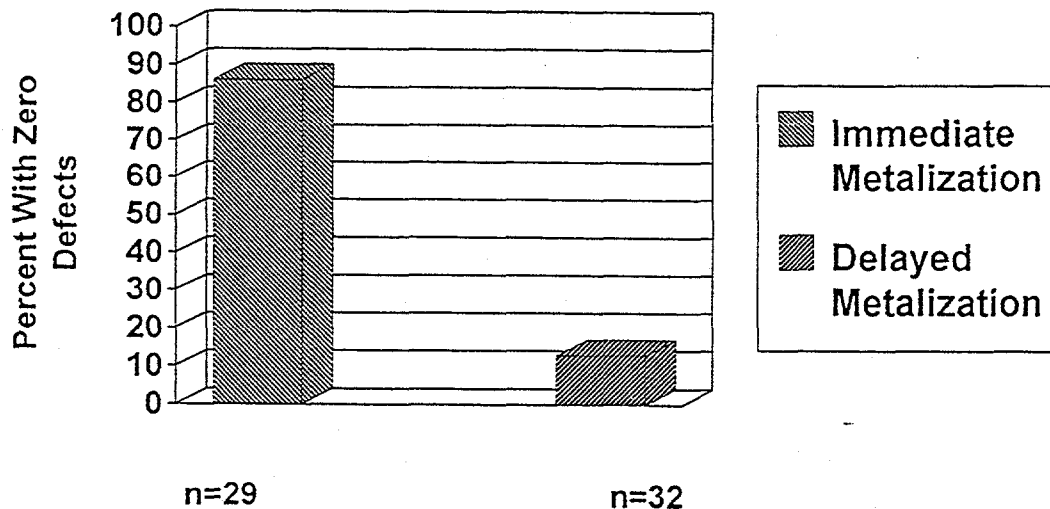


**Figure 4.6.** Shorting defects as a function of delay before metallization. Immediate metallization produces a higher percentage of plates having zero electrical defects.

## 5.0 TASK 4: REAR CONTACT DEPOSITION PROCESS

### 5.1 Introduction

Three separate sputter deposition systems have been used to study the metallization process for triple-junction devices: A small sputter-gun system to evaluate materials and the reactive sputtering parameters on small area diodes, an in-line magnetron system to provide back metallization for modules up to 0.37 m<sup>2</sup> and to test the materials properties of the silicon system and the quality of laser scribes. A large-area six-chamber system will provide state-of-the-art metallization for modules up to 0.56 m<sup>2</sup> and allow testing of manufacturing capability for large-area modules.

### 5.2 Materials Evaluation

Triple-junction modules are currently metallized with a ZnO/silver contact compared to the manufacturing practice of bare aluminum on single-junction devices. The bulk of the environmental data has been established on aluminum-backed devices with the current encapsulant. An experiment was undertaken to quantify the performance differences between silver-backed and aluminum-backed triple-junction devices. A comparison of efficiency, current generated in each layer and quantum efficiency at 800 nm is illustrated in **Table 5.1**.

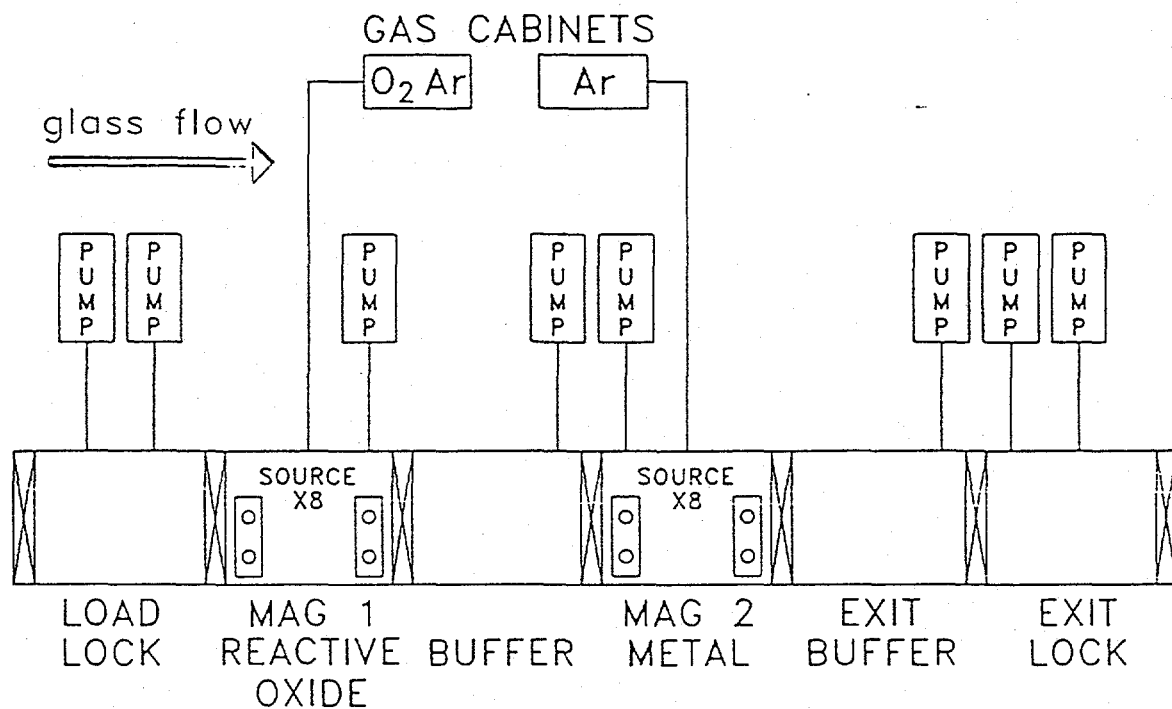
COMPARISON OF ZnO/ALUMINUM AND ZnO/SILVER REAR CONTACTS					
Rear Contact	Efficiency (%)	I-Layer Current (mA/cm <sup>2</sup> )			Quantum Efficiency at 800 nm
		Front	Middle	Back	
ZnO/Aluminum	$\bar{x}$ 8.29	6.06	5.47	4.87	0.164
	$\sigma_x$ : 0.43	0.11	0.07	0.14	0.008
ZnO/Silver	$\bar{x}$ : 9.46	6.05	5.57	5.72	0.237
	$\sigma_x$ : 0.48	0.12	0.06	0.09	0.009
Ratio of <u>Aluminum</u> Silver	0.88	1.00	0.98	0.85	0.69

Table 5.1

The cells made with the ZnO/aluminum rear contact had significantly lower efficiencies than cells made with the ZnO/silver contact because of lower current generated in the back I-layer. The a-Si deposition recipe used in this experiment was optimized for ZnO/silver. If the recipe was optimized for ZnO/aluminum, the loss in efficiency would be less--how much less is not known.

### 5.3 Large-Area Development

A six-chamber metalization system will be used to deposit the oxide/metal layers required for the back contact on triple-junction modules. All of the chambers have been cleaned in preparation for assembly. One chamber required extensive modification to be used as a deposition chamber for the oxide materials. Eight sputtering cathode positions are available for each of the magnetron chambers. The heater configuration and placement in the system has been decided requiring some additional modifications. (Figure 5.1)



**Figure 5.1.** Schematic diagram of magnetron metalization system.

The large-area six-chamber system was facilitated to test the magnetron cathodes in a single chamber. Several aluminum films were deposited on 0.41 m wide glass substrates and measured for thickness uniformity. Results of this test are shown in **Figure 5.2**. Even at locations 1 and 5, which are 0.01 m from the glass edge, the percent deviation from the mean thickness is within 10%.



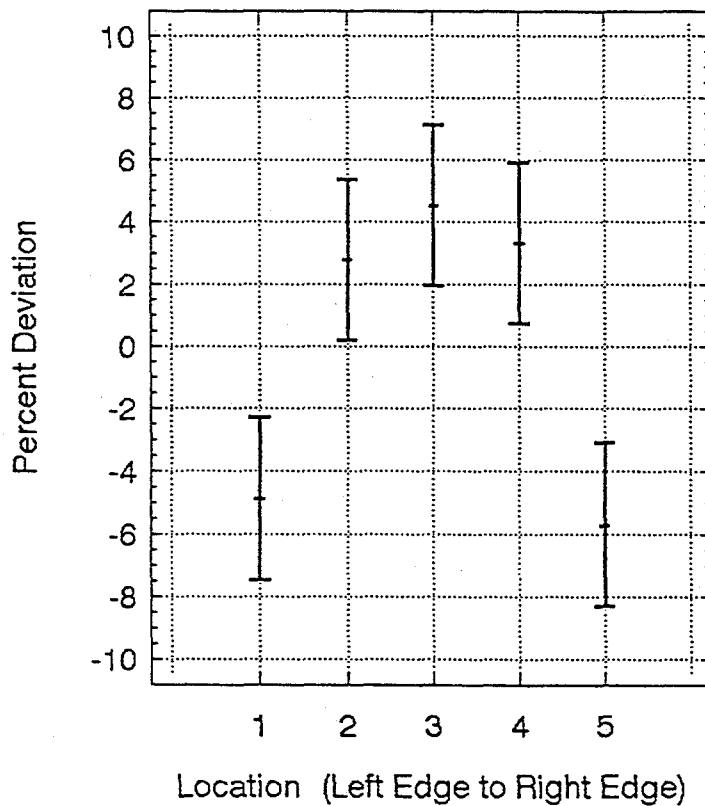


**Figure 5.2.** Aluminum thickness vs. location across the plate. The thickness drops off toward the edges, but overall uniformity is within 10% of the nominal value.

The remaining chambers are being assembled using the heater assemblies currently available to eliminate additional design time. These heaters have been cleaned, refurbished mechanically and rewired to improve reliability. All six chambers have been connected together and their transport mechanisms aligned to permit substrate holder travel through the system. Vacuum plumbing and electrical wiring have been completed and leak-checking is currently in progress.

The bulk of the effort on Task 4 over the last six months has been devoted to preparing a system capable of sputter deposition of an oxide/metal rear contact on large-area substrates.

## **6.0 TASK 5: FRIT/BUS/ENCAPSULATE/FRAME**

### **6.1 Introduction**

The Phase I efforts of Task 5 have focused on three main areas:

First, we specified and procured equipment for the application of conductive frit on large-area modules. Second, we selected an encapsulant for large-area module coverage that is capable of providing wet hi-pot isolation on large-area modules. Third, we worked toward providing a connector that is both low cost and environmentally sound.

The following is a summary of the work to date in these areas.

### **6.2 Large-Area Frit Dispenser**

A three axis motion-controller system was evaluated and chosen for application of the conductive frit used in the bus bar pattern on large-area modules. This system will also be used for laser scribing of large-area modules. An indexer was designed for holding substrates on the gantry system. The concept is an edge holder design which supports the substrate on all four sides. This design has the flexibility to accommodate various size substrates by means of a slide rail adjustment. Flatness of  $\pm .25$  mm ( $\pm 0.01$ " ) can be maintained by adjusting the delrin substrate supports.

An auto-leveling valve system was designed to dispense the conductive frit. The valve system consists of a retainer cartridge, pump and level sensor. Initially an ultrasonic split sensor was used to activate the pump for re-filling. Problems with sensitivity to position, pressure and conditional wet/dry state of attachment were found to be potential causes of failure. A flush mountable capacitive proximity sensor was found to be more reliable and is presently being used.

The fired frit characteristics were optimized through experimenting with various dispensing tip parameters. **Figure 6.1** indicates that a working distance of  $4.0 \pm 1.0$  mm is adequate in maintaining thickness tolerances. Previous systems required working distances of  $\pm 0.03$  mm.

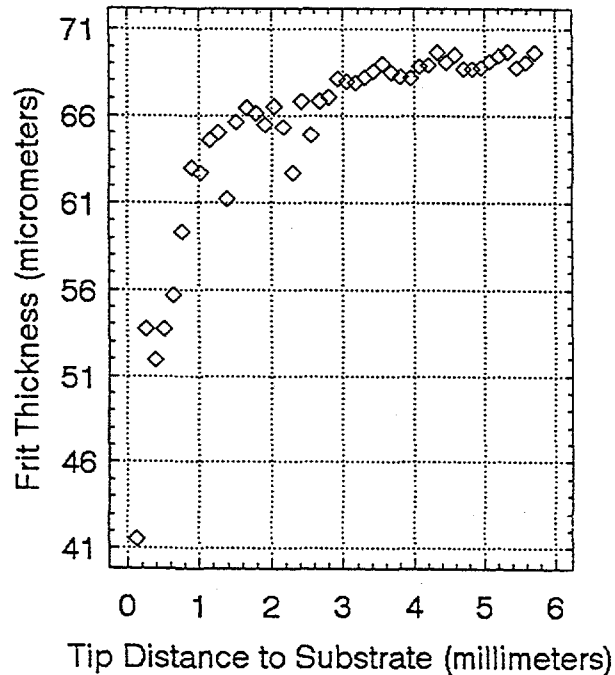


**Figure 6.1.** Bus-bar thickness vs. working distance of the tip from the substrate surface.

Initial samples of low-fired conductor showed evidence of lead metal reduction when fired at a belt speed of 0.61 m/min (24 in/min) in the firing furnace. Subsequent samples fired at 0.46 m/min (18 in/min) had pull strengths of (25 lbs.) after a-Si deposition and heat treatment. Incomplete organic burnout and evidence of lead reduction are problems which have been associated with delamination of the conductive frit. We continue to work with our supplier to improve the frit formulation for our particular process and application. Methods that provide a denser structure to minimize entrapped organics are being tested for improved pull strengths. First

samples fired indicated approximately 30% higher pull strength values. Work continues to optimize this material and process.

### 6.3 Coating

Spray coating studies were conducted to screen candidate materials for application to large-area triple-junction modules. The objective of these studies was to select a coating formulation that was both low in cost and durable enough to pass NREL (SERI/TR-213-3624) Interim Qualification tests.

Seven different formulations were coated onto modules for the evaluations. They can be categorized into 3 main types: polyester/urethanes, acrylic/urethanes and UV curable acrylates.

Evaluations of these coating formulations were performed by using the following test methods:

1. Water Immersion Test per Solarex procedure  
Water immersion at  $50^{\circ}\text{C} \pm 2^{\circ}\text{C}$ , illuminated (ELH light source) for five days.
2. Thermal Cycling - 200 cycles  
233 K to 363 K @50% RH and period not to exceed six hours.
3. Wet Hi-Pot Test as per NREL (SERI/TR-213-3624)
4. UL 1703 Cut Test for hardness.
5. UV Exposure - 1000 hrs.  
QUV  $60^{\circ}\text{C}$  UV/ $40^{\circ}\text{C}$  condense

An acrylic/urethane coating performed best in the screening tests. The most difficult of the tests to pass has been the wet hi-pot. The ability of the coating to withstand the 2250 v was found to be a strong function of the type of encapsulant used (Figure 6.2)

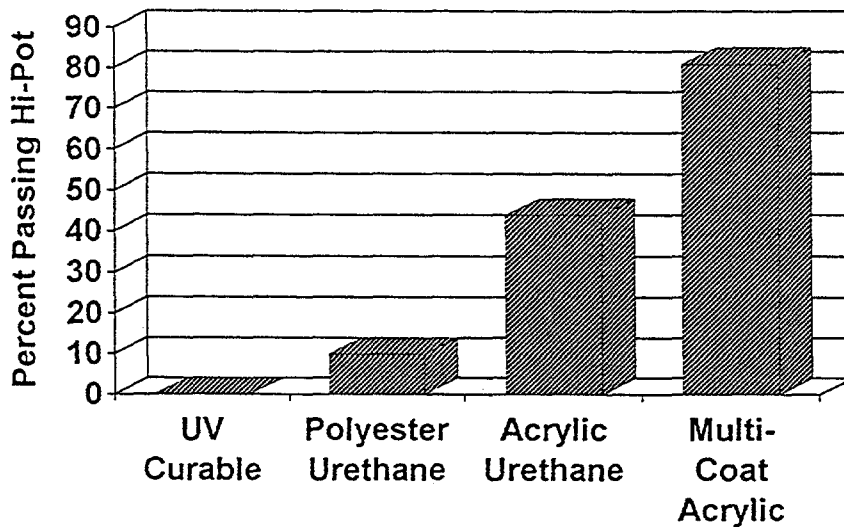


**Figure 6.2.** Comparison of the percentage of plates passing wet hi-pot for modules encapsulated with different materials. All plates were isolated with the wide-isolation scribe.

Focus was given to improving wet hi-pot success to 100%. Failure analysis indicated that pinholes and particulates contributed to low voltage breakdown. De-airing additives were modified to minimize bubble formation during mixing and spray application. Also, laminar flow hoods were used over the load station of the paint spray booth to aid in controlling particulates.

These efforts improved wet hi-pot yields to approximately 50% on 102  $\mu\text{m}$  coatings. Process variations with multiple coats were evaluated in an effort to overcome defect related failures. A three coat process totaling approximately 178  $\mu\text{m}$  improved hi-pot results to >80% yield. The effect of coating thickness on breakdown voltage can be seen in Figure 6.3. Further environmental tests on multi-coat process were begun.

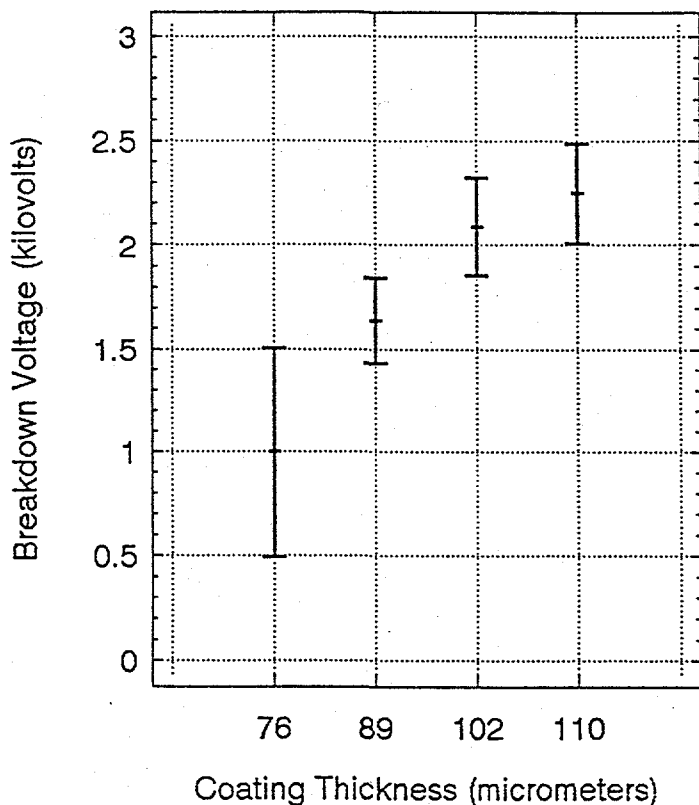


**Figure 6.3.** Breakdown voltage vs. acrylic encapsulant thickness. The breakdown voltage is defined as the voltage at which the module passes  $50 \mu\text{A}$ .

Screening tests indicated that some corrosion and possible film degradation after 1000 hours of UV exposure. Further testing with UV inhibitors and the multi-coating process is on-going. Initial results have been encouraging. Wet hi-pot testing was completed following 50 thermal cycles with all units passing. Humidity freeze and thermal cycling tests continue.

We are also exploring the use of IR spectroscopy as a tool for analysis of the encapsulant formulation. As a monitoring tool IR spectroscopy will be helpful in determining the extent of polymerization that has occurred and the amount of solvent remaining in the encapsulant. It is believed through chemically monitoring the cure process and the mechanical performance of the encapsulant under environmental conditions further improvements in the encapsulant formulation will be achieved.

Other methods of environmentally protecting modules have been explored this past year. One configuration consists of a coated PV Panel attached to a conductive metal backplate with securement clips and a barrier asphaltic sheet between backplate and panel. The environmental advantages initially sought were moisture resistance and an added barrier to environmental stress and UV radiation. All units with this configuration passed wet hi-pot testing. Related testing of this configuration of packaging indicated more resistance to breakage. Test panels failed to break when dropped from a height of 0.9 m (36 in.) onto a concrete surface. Additionally, the metal backplate and clips could function as an internal ground providing a safety advantage. Efforts are underway to deploy outdoor test panels with this configuration for observation.

Finally, several types of UV curable coating materials have been screened. Advantages with a 100% solids coating system are increased production rates and less expensive processing costs. The environmental test results (thermal cycle, humidity freeze and water immersion) of UV curable coatings screened to date indicate that they can provide good adhesion and moisture resistance, but the thermal stability and UV resistance of the coating need to be addressed to provide a good coating for PV modules.

#### **6.4 Connector**

Our primary objective in the development of a connector for thin-film photovoltaic (TFPV) modules is to provide a reliable, surface-mounted connector with environmental integrity.

Several types of connectors were initially investigated. They included J-Boxes, in-line connectors, single lug type connectors and hi-voltage connectors. Due to cost considerations and difficult environmental test conditions the hi-voltage connector seemed best suited toward meeting this objective.

Initial testing involved subjecting the hi-voltage connector to a two week exposure of humidity soak (85°C/85RH), then submersing the connector in 12.7 mm (5 in) of water and hi-pot tested @2250 V<sub>DC</sub> for a period of one minute. Results indicated that 9 sets, 18/20 individual connectors, passed this severe test.

Based on these results efforts were taken to reach a confidential disclosure agreement with the connector manufacturer. This agreement would enable the connector manufacturer and Solarex to collaborate on the design of a specific connector capable of passing the tests required to make it acceptable for high voltage (600 V) PV arrays.

A preliminary list of electrical, mechanical and environmental connector requirements was submitted to the connector manufacturer by Solarex. This design phase is in progress and a conceptual design will be available shortly.

Efforts to evaluate attachment equipment for automation of this process will be delayed until final connector design has been determined.

## **7.0 TASK 6: MATERIALS HANDLING**

### **7.1 Introduction**

This team's efforts were directed at completing a layout of equipment, based on current processing techniques, which would be capable of producing ten megawatts of multi-junction thin film photovoltaic modules. Individual pieces of equipment will now be analyzed to determine facilitation, incoming materials and effluent handling requirements for producing a volume of 10 megawatts of large-area high efficiency multi-junction modules.

Interim manual materials handling techniques to produce prototype large-area modules have been designed and implemented.



## **7.2 Ten Megawatt Plant Layout**

The equipment layout for a prototypical thin film multi-junction photovoltaic module plant was completed (See **Figure 7.1**). Inputs from each of the PVMaT task teams as to their equipment requirements was gathered by the Task 6 team and a possible equipment layout was designed based on their current level of experience.

## **8.0 TASK 7: ENVIRONMENTAL TEST, YIELD AND PERFORMANCE ANALYSIS**

### **8.1 Introduction**

The task activities during this initial phase of the manufacturing technology program have emphasized the design and development of environmental and electrical testing capabilities and an electrical cure processing station for large-area triple-junction a-Si modules. This emphasis has been included on the design and fabrication of a light-soak station and electrical test station capability for large-area modules (up to 0.74 m<sup>2</sup> (8 ft<sup>2</sup>)) and expansion of environmental test area to accommodate a new Hi-Pot test station. In addition, characterization of the electrical cure characteristics of triple-junction a-Si modules has been pursued along with the design of a station capable of electrically curing large-area modules.

### **8.2 Light-Soak Station**

Evaluating the susceptibility of large-area modules to light-induced effects is of primary concern as new processing methods are developed over the course of the program. The assembly of an appropriate light-soak station early in the program is essential.

Considerations in the design and fabrication of the light-soak station include the type of light source, its spectral content relative to absorption in the individual junctions of the triple-junction structure, and the considerable size of the modules to be tested. The station has been sized to accommodate up to an 0.74 m<sup>2</sup> (8 ft<sup>2</sup>) module.

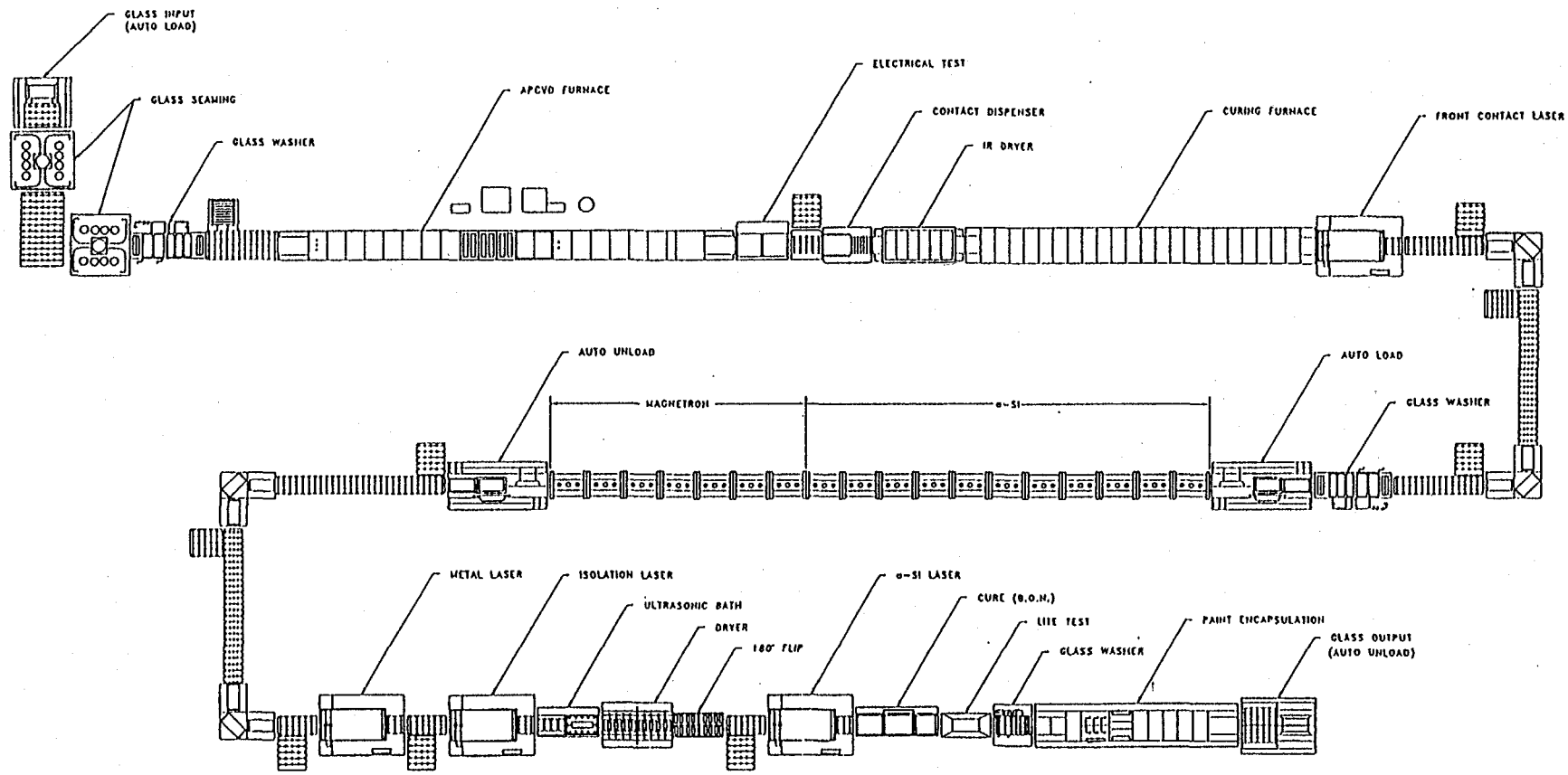


Figure 7.1. The 10 megawatt plant layout.

Investigations were made of available light sources which might closely approximate the DC 5500°C solar source. A review of several papers in the literature provided little direction on the use of light sources to soak triple-junction devices. Some stage lights with temperatures near 5500°C may be available but are judged to be expensive in operation and maintenance. DC argon arc lamps are also high cost and still have a spectral content which is not ideal. Sodium vapor lamps which have been used for indoor light-soaking of single-junction a-Si have a high spectral content in the yellow and potentially would imbalance the middle-junction in the triple-junction structure.

A separate study has been conducted comparing the light-induced effects on triple-junction panels exposed outdoors against similar panels exposed on sodium vapor lamps. The results of this investigation show that there are some differences in light-induced effects between the two methods. These differences are not as great as would have been expected. At exposure times on the order of 1000 hours or greater the two methods differed by only a few percentage points.<sup>1</sup> As a result of these data the decision was made to proceed using the sodium vapor lamp as the light source for the large-area light-soak station.

The light-soak station design evolved following this analysis is comprised of eleven high-pressure sodium lamps arranged in an array to illuminate the area of interest under a support structure for the panels (**Figure 8.1**). The standard GE lamp reflectors were coated with a Kodak white reflectance coating to enhance the uniformity of light intensity across the array. The height of the support structure above the lamps was adjusted to provide a nominal light intensity of one sun. The panel support structure itself is comprised of a steel base and side rails on which glass panes are placed. Module temperature control is achieved using two large fans to circulate air over the unit.

---

<sup>1</sup>Newton, James A. "Comparison of Amorphous Silicon Degradation Under Various Light Sources", NREL Photovoltaic Performance and Reliability Workshop, Golden, CO, September 1992.

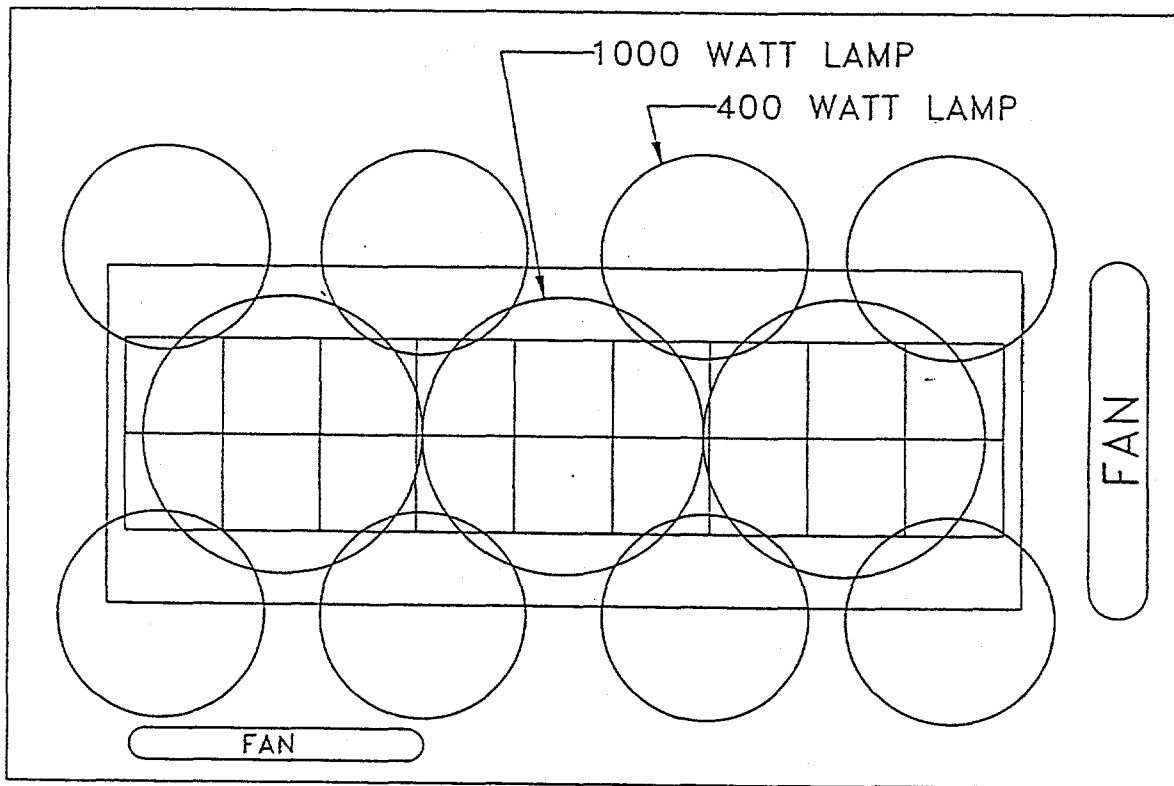


**Figure 8.1.** The layout of the large-area light-soak station.

The importance of maintaining temperature control in order to achieve reproducible light-soak results is demonstrated in **Figure 8.2**. This data collected on very thick a-Si (highly susceptible to light-induced effects) shows output increasing by about 14 percent as the temperature of the devices under light-soak is increased from 35°C to 75°C. Temperature control was established as one of the design criteria for the light-soak station.

The lamp configuration is shown in **Figure 8.3**, along with the temperature and illumination mapping of the station. A mapping of the illumination characteristics of the station is shown in **Figure 8.4**. In designing the station, objectives of maintaining the temperature at less than 50°C and the light intensity within 30% of one sun were adopted. This figure shows these objectives were met. The illumination (**Figure 8.4**) was mapped using the short circuit current of an 0.04 m<sup>2</sup> a-Si reference module as

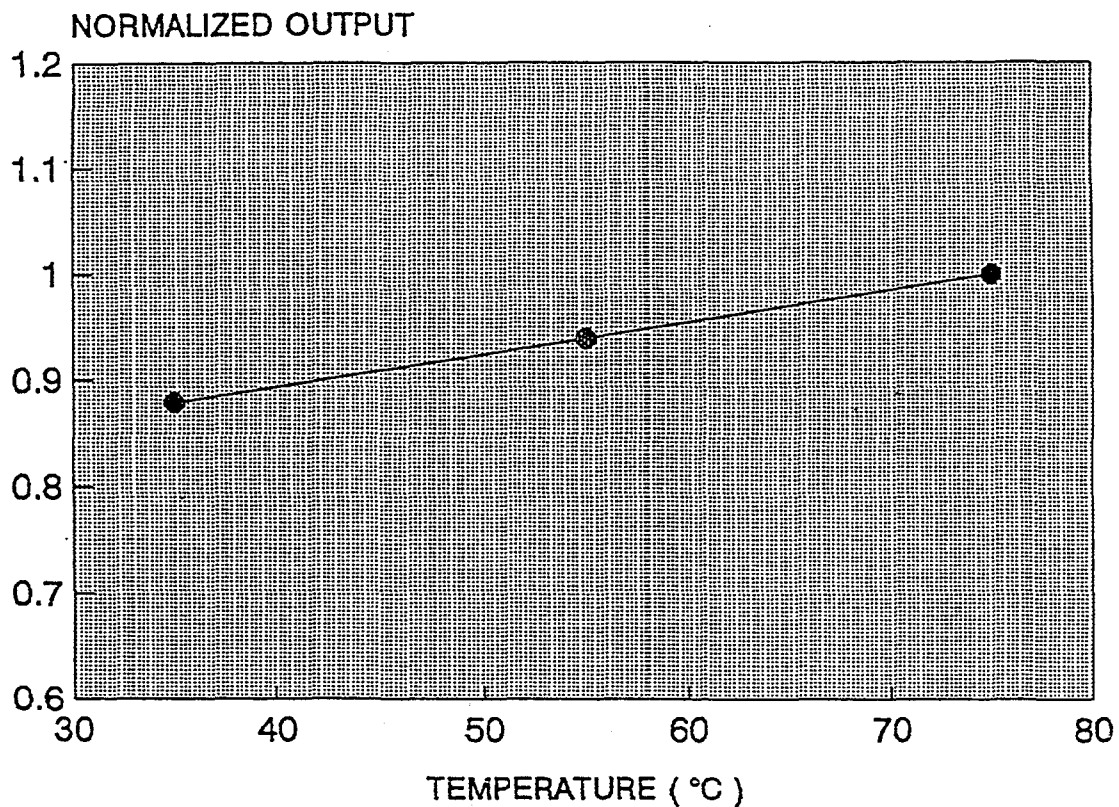


**Figure 8.2.** Impact of temperature on light-induced defects of a-Si modules. The data is based on 100 hour light-soak using sodium vapor lamps.

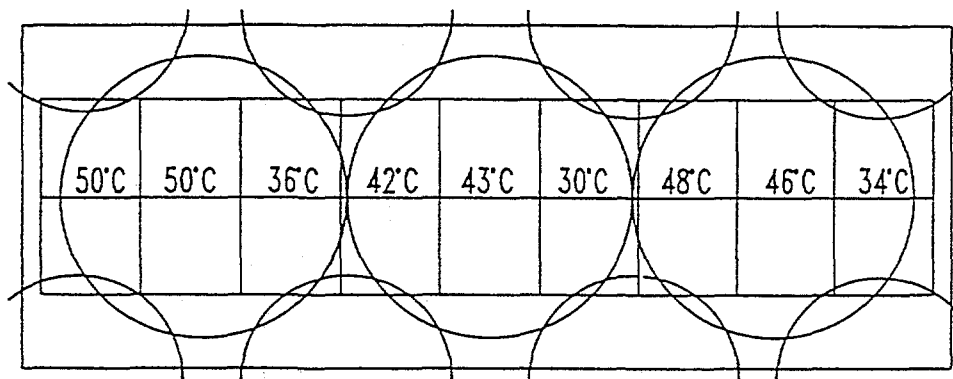


**Figure 8.3.** The temperature map for the large-area light-soak station.

measured on a Spire simulator. The illumination values shown on the figure are normalized relative to this measured short circuit current. The temperatures were measured by placing six 0.1 m<sup>2</sup> modules with thermocouples attached down the center of the illuminated area. The temperatures were recorded after 60 minutes of illumination.

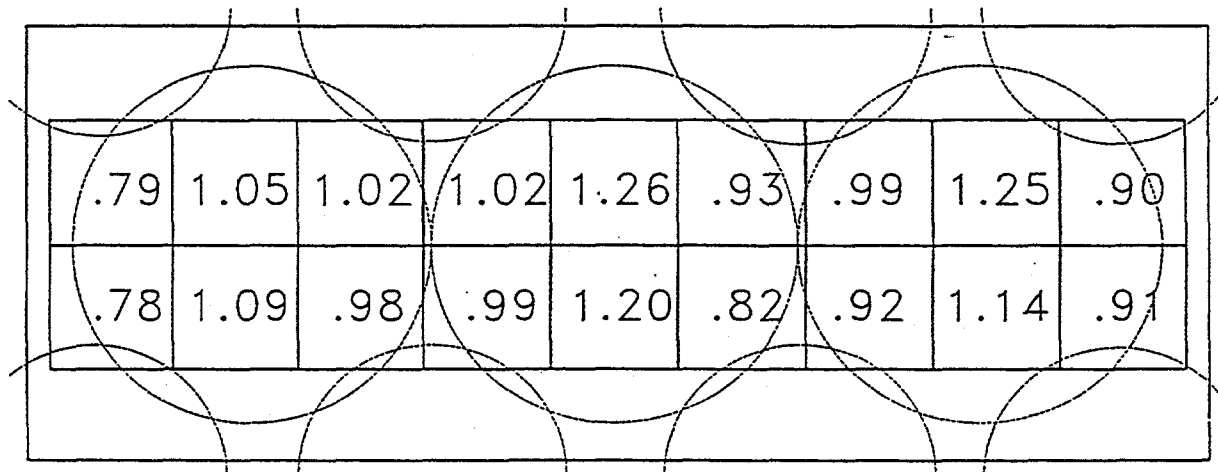


**Figure 8.4.** The light intensity map for the large-area light-soak station.

### 8.3 ENVIRONMENTAL TEST

Efforts have been initiated to provide the capability for environmental testing of large-area triple-junction modules to meet the requirements of the Interim Qualification Tests and Procedures for Terrestrial Photovoltaic Thin-Film Flat-Plate Modules. This test capability is intended to provide the means to follow the interim plan explicitly except that a static load mechanical test capability will be provided in place of the dynamic mechanical load test.

The necessity of handling large-area product and the larger size of the test equipment for it, demand the expansion of the facilities for these purposes. A significant effort has been expended to determine the space requirements for the test area and the layout of the equipment within this area. The result has been the increase in the size of the testing facility of 28 per cent.

The testing capability has been advanced to include the tests listed below for large-area modules of at least 0.56 m<sup>2</sup> (6 ft<sup>2</sup>) in size. We augmented our test capabilities by adding a wet insulation resistance test and a megger test to be used for outdoor wet insulation resistance testing.

Large-area test capability:

- Thermal cycle test
- Humidity freeze cycle test
- Electrical insulation test (Dry hi-pot)
- Hail impact test
- Wet insulation resistance test

The design considerations for the Hi-pot tests station include the capability to immerse any edge of a test module up to 1.83 m (6 ft.) long in an aqueous solution, wet the entire module and safely apply a potential of 2250 volts to the module. The design approach chosen for the station uses a grounded steel frame-work and an inner enclosure of heavy gauge non-conductive polymeric materials. These polymeric materials are attached to the support structure using only non-conductive fasteners. Interlocks are used to ground all test voltages when the enclosure is open and heavily insulated lead wires are run from the test instrument. The prescribed surfactant-water solution is pumped to the enclosure from a supply reservoir and applied to the module from all sides through a series of small orifices.

## 8.4 ELECTRICAL TEST

Consideration has been given to the light sources which might be used for electrical testing of triple-junction a-Si modules. The review included pulse simulators such as LAPS units which require large-areas to set up and are expensive to purchase and maintain. In addition, the experience with thin film modules is that special adaptations need to be made to compensate for capacitive reactance of the modules which affects the measured output curve during the very short duration of the light pulse. Spire simulators, which are available at Solarex and NREL, have been used to test a number of triple-junction submodules with reasonable results. It appeared that with proper reference cells and calibration, a Spire type simulator would be adequate for the electrical measurement of large-area a-Si modules.

The work proceeded with the one-sun simulator available at Solarex based on this analysis. The initial task was to raise the bonnet of the tester about 25 mm to provide space in which to insert large-area modules. We mounted fixturing to support the module and carry it into the illuminated area in this space under the bonnet. This fixturing was sized to hold large-area modules up to 1.83 m (6 ft.) in length.

The bonnet of the tester was subsequently modified to allow illumination of this long panel. Sections of the lower part of the bonnet were removed and formed extension hoods attached to shade the test module from exterior lighting. Measurements taken to map the illumination intensity over the area required for a large-area module were quite uniform except at the very extremes of the module length. The mapping was conducted using an  $0.07 \text{ m}^2$  sub-module by measuring the short circuit current. **Figure 8.5** illustrates the mapping results on a normalized basis with the nominal intensity value being 87 per cent of the peak value. The implementation of further modifications is being considered to improve the illumination uniformity over the full area of the fixturing.



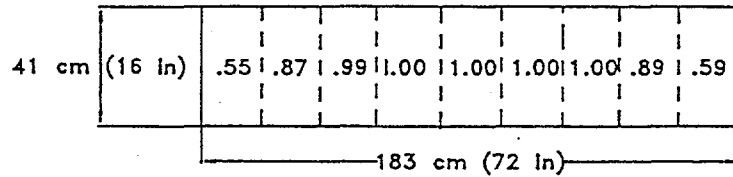


**Figure 8.5.** The normalized illumination intensity map of the modified large-area electrical test station. The total area neon illumination was measured at 0.877 using a single-junction reference cell.

## 8.5 ELECTRICAL CURE

The application of reverse bias electrical voltage to thin-film a-Si diodes to "cure" minor film defects has been a common practice on single-junction modules. The objective in the current program is to determine the reverse bias electrical parameters that apply to large-area triple-junction modules and design the process to implement them. Available triple-junction 0.1 m<sup>2</sup> submodules fabricated in at least three different deposition systems have been evaluated for necessary and tolerable reverse bias voltage and current requirements. Early measurements recorded indicated voltage tolerances for the triple-junction modules with silver back contact metal may be on the order of one volt lower than for single-junction modules with aluminum back contact metal. However, more recent results indicated voltages higher than those applied to single-junction modules are more effective in curing the triple-junction devices.

Fixturing for electrical curing of panels has been used to compare an electronic cure of triple-junction submodules with a manual cure method. In the electronic cure a charged capacitor is used to reverse bias the module segments. In this case high instantaneous currents can be delivered to any defect which may be present. In the

manual cure procedure voltage from a power supply is applied starting from zero and increasing to a set level by turning a pot adjustment by hand. The manual cure method has been viewed as a reference or base method and was used in this comparison because it was feared that the automatic, electronic cure method might cause damage to triple-junction devices. We reasoned that the voltage-current surge may cause break-down and subsequent residual defects in the thinner junctions of the multi-junction semi-conductor devices. (The manual cure is characterized by a gradual increase in voltage and current.)

The results of these tests, as shown in **Figure 8.6** and **Figure 8.7**, indicate that the electronic cure method is as good or better in curing defects in triple-junction panels than the manual cure method. The data for these figures was gathered by electrically testing groups of panels at AM 1.5 Global before and after each electrical cure procedure. The final cure referred to on each of the figures is a second manual cure. The curves are normalized in that after the output is measured after the final manual cure, the modules are assumed to be at 100% of potential output.

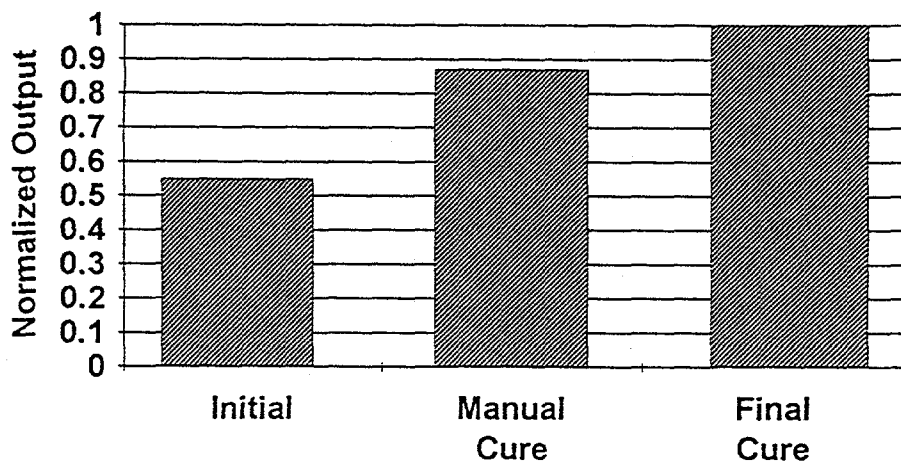


**Figure 8.6.** Manual electrical cure of triple-junction modules. Shown are the initial average power output, the average power output after manual cure and the average power output after final cure.

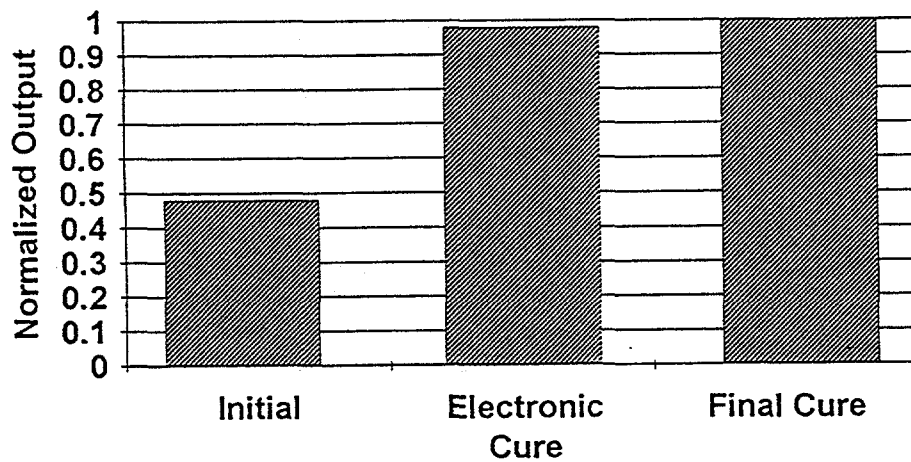


**Figure 8.7.** Automatic electrical cure of triple-junction modules. Shown are the initial average power output, the average power output after the automatic electrical cure, and the average power output after final cure.

<b>Document Control Page</b>	<b>1. NREL Report No.</b> NREL/TP-411-6047	<b>2. NTIS Accession No.</b> DE94000249	<b>3. Recipient's Accession No.</b>
<b>4. Title and Subtitle</b> Large-Area, Triple-Junction a-Si Alloy Production Scale Up		<b>5. Publication Date</b> January 1994	
<b>7. Author(s)</b> R. Oswald, J. O'Dowd		<b>6.</b>	
<b>9. Performing Organization Name and Address</b>  Solarex Thin Film Division 826 Newtown-Yardley Road Newtown, PA 18940		<b>8. Performing Organization Rept. No.</b>	
		<b>10. Project/Task/Work Unit No.</b> PV450101	
		<b>11. Contract (C) or Grant (G) No.</b>  (C) ZM-2-11040-2  (G)	
<b>12. Sponsoring Organization Name and Address</b> National Renewable Energy Laboratory 1617 Cole Blvd. Golden, CO 80401-3393		<b>13. Type of Report &amp; Period Covered</b>  Technical Report 17 March 1992 - 18 March 1993	
<b>15. Supplementary Notes</b> NREL technical monitor: R. Mitchell		<b>14.</b>	
<b>16. Abstract (Limit: 200 words)</b>  This report describes work under a 3-year subcontract to advance Solarex's photovoltaic manufacturing technologies, reduce its a-Si:H module production costs, increase module performance, and expand its commercial production capacity. Solarex will meet these objectives by improving the deposition and quality of the transparent front contact, optimizing the laser patterning process, scaling up the semiconductor deposition process, improving the back-contact deposition, and scaling up and improving the encapsulation and testing of its a-Si:H modules. During Phase 1, Solarex focused on (1) scaling up components of the chemical vapor deposition system for deposition of the front contact, (2) scaling up laser scribing techniques, (3) improving triple-junction recipes for module production, and (4) improving metal oxide back contacts. This work resulted in adapting portions of the manufacturing line to handle substrates larger than 0.37 m <sup>2</sup> .			
<b>17. Document Analysis</b> a. Descriptors large area ; amorphous silicon ; manufacturing ; modules ; chemical vapor deposition ; laser scribing ; photovoltaics ; solar cells  b. Identifiers/Open-Ended Terms  c. UC Categories 270			
<b>18. Availability Statement</b> National Technical Information Service U.S. Department of Commerce 5285 Port Royal Road Springfield, VA 22161		<b>19. No. of Pages</b> 51	
		<b>20. Price</b> A04	